

# STATUS OF ELECTRON BEAM SLICING PROJECT AT NSLS-II, BNL\*

A. He, F. Willeke, L.H. Yu, BNL, Upton, NY 11973, USA

## Abstract

The Electron Beam Slicing (e-beam slicing) at NSLS-II, Brookhaven National Laboratory, supported by the Laboratory Directed Research and Development (LDRD) Program, is focused on the development of the new method to generate ultra-short x-ray pulses using focused short low energy ( $\sim 20$  MeV) electron bunches to create short slices of electrons from the circulating electron bunches in a storage ring. The e-beam slicing activities are staged in 3 main phases. In Phase 0, the theory of e-beam slicing is developed, the low energy linac compressor is simulation designed, the radiation separation between the satellite and core is analyzed by simulation and the properties of the e-beam slicing system are discussed and compared with other ultra-short x-ray sources. In Phase I, the crucial parts of the e-beam slicing scheme will be tested experimentally which include the micro-focusing test of low energy electron beam in space charge dominated regime and the electron beam slicing test using the Accelerate Test Facility (ATF) electron beam as the high energy beam. The kick back system will be simulation designed to increase the repetition rate of e-beam slicing system. At Phase II, the design of e-beam slicing project at NSLS-II will be proposed. Phase 0 has completed successfully, Phase 1 is under way. This paper presents an update on the status of Phase 0.

## INTRODUCTION

The community interested in science using sub-picosecond x-ray pulses is growing rapidly. Laser slicing is one of the approaches to generate ultra-short x-ray pulse [1–6]. Typically, for laser slicing the x-ray pulses are of the order of 100 fs with repetition rate of order of 1 kHz and the number of photons per 0.1% bandwidth per pulse is of the order of 1000. To generate ultra-short x-ray pulses with many orders of magnitude higher repetition rate, another method is proposed by Zholents [7, 8] using a crab cavity which provides pulse length of order of a picosecond. It provides a continuous stream of x-ray pulses [9] with a much higher average flux. A new source of ultra-short x-ray pulses is x-ray free electron laser, with the pulse energy many orders of magnitude higher than storage ring and pulse width of 100 fs or less [10]. However, compared with the storage ring sources, the fluctuation of the intensity and wavelength from a SASE FEL is large, and, the repetition rate is low. For example, the repetition rate of LCLS SASE FEL is 120 Hz [11]. Hence, even though the single pulse energy is much lower than the SASE FEL pulse, the high repetition rate and high pulse to pulse stability of storage ring sources continue to attract a wide range of user interests.

The electron beam slicing method [12, 13] is a different approach to generate ultra-short x-ray pulses of the order of 100 fs pulse length. As shown in Fig. 1, when a short electron bunch from a low energy linac (for example, 20 MeV, 200 pC, 150 fs) passes 35  $\mu\text{m}$  above a storage ring bunch (30 ps) at a right angle, it kicks a short slice ( $\sim 160$  fs) of electron bunch vertically. The radiation from the short slice is separated from the core bunch. This method has many advantages, i.e., small space in storage ring for interaction, very short radiation pulse length ( $\sim 160$  fs), high pulse flux, high repetition rate and high stability. We expect the new method may provide a complimentary approach to other ultra-short x-ray pulse sources.

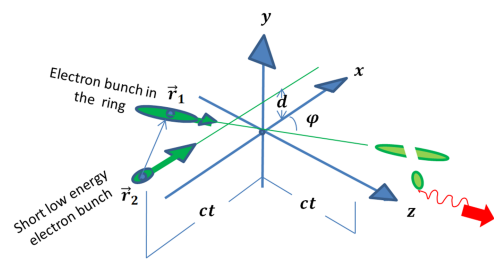


Figure 1: Illustration of electron beam slicing.

## THEORY OF E-BEAM SLICING

We explored the new method by calculating the angular kick received by a high energy electron (labeled as bunch 1), generated by a point charge in the low energy linac electron bunch (labeled as bunch 2) and integrated over the 3-D electron distribution of the low energy bunch. The result gives the angular kick as a function of the 3-D position of an electron in the storage ring bunch:

$$\Delta\theta_y = \frac{eq_2 Z_0 c}{2\pi E_1} \frac{\gamma_2(1 - \beta_1\beta_2 \cos \varphi)}{\sqrt{\gamma_2^2(1 - \cos \varphi)^2 + \sin^2 \varphi}} \frac{1}{\sqrt{2}\sigma_y} \times f_y(\rho, \bar{u}_1, \bar{y}_1) \quad (1)$$

where  $f_y$  gives the profile as a function of the high energy electron's position

$$f_y(\rho, \bar{u}_1, \bar{y}_1) = \int_0^\infty \text{Re}[W(\bar{u}_1 + iy)][e^{-(\rho y - \bar{y}_1)^2} - e^{-(\rho y + \bar{y}_1)^2}] dy \quad (2)$$

\* Work supported by DOE under contract LDRD12-023 and LDRD14-022

with

$$\begin{aligned} \rho &\equiv \sqrt{\frac{\gamma_2^2}{\gamma_2^2(1 - \cos \varphi)^2 + \sin^2 \varphi} \cdot \frac{\sigma_x^2 \sin^2 \varphi + \sigma_z^2(1 - \cos \varphi)^2}{\sigma_y^2}} \\ \bar{y}_1 &\equiv \frac{d - y_1}{\sqrt{2}\sigma_y} \\ \bar{u}_1 &\equiv \frac{z_1 \sin \varphi + x_1(1 - \cos \varphi)}{\sqrt{2\sigma_x^2 \sin^2 \varphi + 2\sigma_z^2(1 - \cos \varphi)^2}} \end{aligned} \quad (3)$$

$E_1$  is the energy of the storage ring electron 1,  $\varphi$  is the crossing angle between the beam axis of the low energy bunch and the beam axis of the high energy bunch, while  $d$  is the vertical distance between the centres of the low energy beam and the high energy beam.  $x_1, y_1, z_1$  are the coordinates of the high energy electron,  $\sigma_x, \sigma_y, \sigma_z$  are the RMS beam size of the low energy bunch.  $q_2$  is the charge of low energy bunch,  $\gamma_2$  is its dimensionless energy,  $Z_0 = 377 \Omega$  is the vacuum impedance.  $W$  is the error function:  $W(u) = e^{-u^2} \text{erfc}(-iu)$ . Eq. (1) gives the angular kick as a function of the electron's 3-D position  $x_1, y_1, z_1$  in the storage ring bunch 1. The profile function Eq. (2) describes the profile of the slice bunch and can be used to estimate the pulse width of the slice [14].

## BUNCH COMPRESSOR SIMULATION

The estimated examples [12–14] show to obtain the sufficient angular kick to separate the slicing from the core, very short ( $\sim 150$  fs), focused ( $\sim 35 \mu\text{m} \times \sim 35 \mu\text{m}$ ), high charged (50 pC  $\sim$  200 pC) bunch is required. To reduce the cost, we simulation designed a 5 MeV bunch compressor using BNL photo-cathode electron RF-gun to generate a low energy bunch with the 166 fs RMS bunch length, 28  $\mu\text{m}$  and 31  $\mu\text{m}$  RMS beam size in the vertical and horizontal direction separately, with 50 pC charge [15]. To increase the repetition rate of e-beam slicing system, we carried out a simulation study to design a system consisting of the LBNL's VHF gun operating at 186 MHz with repetition rate of 1 MHz [16], superconducting rf cavity at 1.3 GHz, several solenoids and a compressor chicane with a matching section. The simulation code used is IMPACT-T [17]. To check the effect of the Coherent Synchrotron Radiation (CSR), we compared the simulation results with the results when the CSR effect is turned off in IMPACT-T, and also compared with simulation using the code PARMELA which does not take CSR into account [15]. Our comparison shows that the CSR effect is negligible in our case. We carried out a multi-objective optimization procedure using the genetic algorithm [18]. Some optimized results are shown in Table. 1. For example, at 20 MeV with 200 pC charge and a 8.7 m compressor chicane, the optimization leads to 148 fs RMS bunch length at the focal point with 46  $\mu\text{m}$ , and 25  $\mu\text{m}$  for horizontal and vertical RMS beam size respectively. Fig. 2 shows the histograms of 6-D phase space at the final focus point of the compressor

with the color bar indicating the particle density. A more detailed description is to be found in [19].

Table 1: Performances of Compressor

Case	Charge [pC]	Energy [MeV]	$\sigma_L^a$ [fs]	$\sigma_H^b$ [ $\mu\text{m}$ ]	$\sigma_V^c$ [ $\mu\text{m}$ ]
1	150	18	130	47	28
2	200	20	148	46	25
3	200	22	128	42	25

<sup>a</sup> the longitudinal rms bunch length of the linac bunch

<sup>b</sup> the horizontal rms beam size of the linac bunch

<sup>c</sup> the vertical rms beam size of the linac bunch

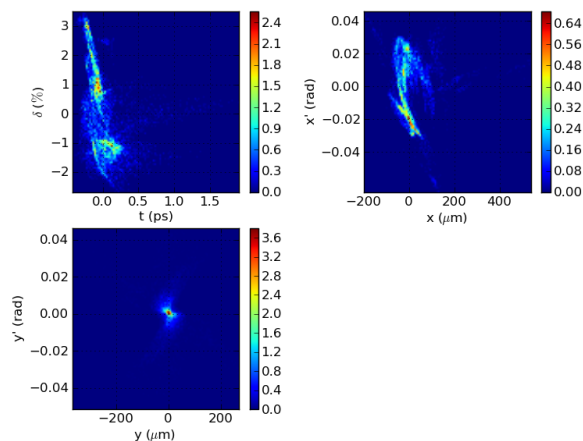


Figure 2: The histograms of 6-D phase space at the final focus point of the compressor. The color bar shows the particle density.

## PHOTON FLUX AND REPETITION RATE

If we use a 20 mm period in-vacuum-undulator of NSLS-II as the radiator [20], the photon flux for 8 keV x-rays is  $10^{15}$  photons/sec/0.1%BW for a beam current 500 mA. With about 1000 bunches, bunch current is 0.5 mA. As an estimate, for a slice of 0.3 ps out of the 30 ps core bunch length, the slice fraction is 0.3 ps/30 ps=1%. Since revolution time is about 2.6  $\mu\text{s}$ , the single pulse photon flux is  $10^{15} \times 0.3 \text{ ps}/30 \text{ ps} \times 2.6 \mu\text{s}/1000 = 2.6 \times 10^4$  photons/0.1%BW. If we choose a camshaft current of 3 mA, the flux can be increase to  $15.6 \times 10^4$  photons/0.1%BW.

The emittance increase sets the limitation on the repetition rate. For a single bunch, the emittance increase due to angular kicks is equal to the emittance increase rate times the damping time. One angular kick of  $5\sigma_y'$  with a slice of 300 fs in a 30 ps bunch increases  $\varepsilon_y$  by  $12\% \varepsilon_y$ . With a repetition rate of 100 Hz for a single bunch, and damping time of 10 ms, the emittance increase is  $12\% \varepsilon_y$ . If we distribute the kicks uniformly over all 1000 bunches, the repetition rate would be 100 kHz. For 100 kHz repetition rate, the photon flux is  $2.6 \times 10^9$  photons/sec/0.1%BW for the example above.

For most synchrotron light source users, the requirement on vertical emittance is not very stringent. Thus depending on the tolerance of the vertical emittance increase, the repetition rate limit can be 100 kHz to 1 MHz at the expense of a slightly reduced separation for the same kick.

## SPECIFIC EXAMPLE

### Slice Profile at Licker and Radiator

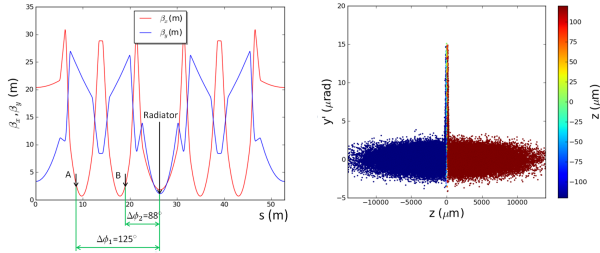


Figure 3: NSLS-II lattice (left). Phase space for  $y'$  versus  $z$  at the crossing point at 8.3 m right after the kick (right).

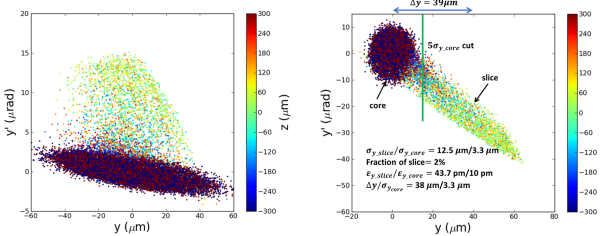


Figure 4: Phase space for  $(y, y')$  at the crossing point right after the kick (left) and at the radiator (right).

We use the 6-D phase distribution shown in Fig. 2 for the low energy bunch from the linac compressor simulation as an example to calculate the slice profile. The formula for angular kick gives the optimum vertical distance from the linac beam to the storage ring beam as  $35 \mu\text{m}$ . To improve angular separation of the slice from the core, we should choose the crossing point in the storage ring with maximum  $\beta_y$  to minimize the core vertical divergence. In the meantime, to reduce the slice pulse length, we need to minimize  $\beta_x$ . This criterion leads us to choose the slicing point at the position of either about 8.3 m (point A) or 19.3 m (point B) in the left plot of Fig. 3 where  $\beta_x = 3.8 \text{ m}$ ,  $\beta_y = 25 \text{ m}$ . These two positions have vertical betatron phase advances from the radiator U20 at position 26 m of about  $125^\circ$  and  $88^\circ$  respectively. Using the 6-D distribution of the linac bunch at the final focus point shown in Fig. 2, we calculate the angular kick received by particles in the storage ring bunch after the crossing and plot the phase space distribution. In the right plot of Fig. 3 we show the phase space for  $y'$  versus  $z$  right after the kick with crossing point at 8.3 m. In the left plot of Fig. 4, we show  $y'$  versus  $y$  at the crossing point at 8.3 m, right after the kick. The right plot of Fig. 4 gives the phase space plot of  $y$  versus  $y'$  at the radiator at 26 m. The right

plot of Fig. 3 shows a thin slice is kicked up right after the crossing, while the left plot of Fig. 4 shows how the slice is separated from the core in  $(y, y')$  phase space, right after the kick. The right plot of Fig. 4 shows the same phase space after a  $125^\circ$  phase advance at the radiator. The transport of phase space distribution is carried out by the tracking code "ELEGANT" [22]. The phase space rotation is such that the slice can be separated from the core both angularly and spatially.

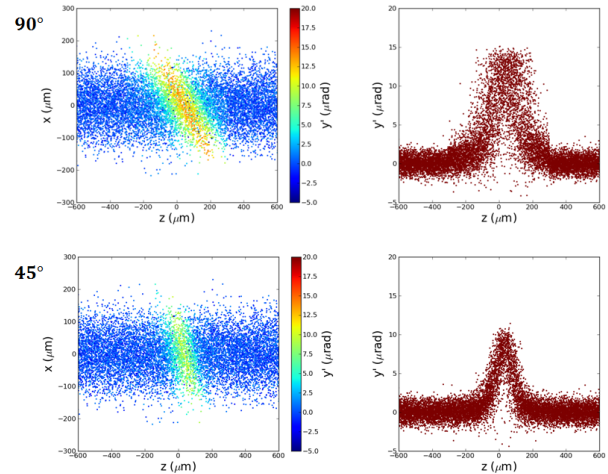


Figure 5: Compare phase space distribution in  $(z, x)$  plane and  $(z, y')$  plane for  $90^\circ$  and  $45^\circ$  respectively.

Table 2: Quantitative Comparison of  $90^\circ$  and  $45^\circ$  Crossing Angle

	$\sigma_t$ [fs]	$\frac{\sigma_{y,\text{slice}}}{\sigma_{y,\text{core}}}$ [ $\mu\text{m}/\mu\text{m}$ ]	slice fraction [%]	$\frac{\epsilon_{y,\text{slice}}}{\epsilon_{y,\text{core}}}$ [pm/pm]	$\frac{\Delta y}{\sigma_{y,\text{core}}}$ [pm/pm]
$90^\circ$	320	12.5/3.3	2	43.7/10	38/3.3
$45^\circ$	150	7.03/3.3	1	22/10	29/3.3

The RMS slice length in this case is 320 fs, much larger than the linac bunch length of 128 fs. This is because the horizontal crossing time at the interaction point at 8.3 m in Fig. 3. It is possible to reduce the pulse length due to the crossing time by reducing the crossing angle [14]. The simulation shows the bunch length is reduced to 150 fs at the expense of only a small reduction of spatial separation from  $38 \mu\text{m}$  to  $29 \mu\text{m}$ . In Fig. 5 we compare the phase space distribution for the  $90^\circ$  crossing and  $45^\circ$  crossing. The left plot is for the  $(z, x)$  phase space with the colour scale representing the kick angle, clearly showing the tilted distribution for the case of  $90^\circ$  gives longer pulse length in  $z$  direction. In the right of the plot we give the distribution in  $(z, y')$  plane, showing clearly the reduction of pulse length for  $45^\circ$  crossing. Table 2 gives the comparison of quantitative analysis of these two cases. The RMS pulse length of the slice is reduced from 320 fs to 150 fs when crossing angle is  $45^\circ$ .

Table 3: Separation Performances of Hard X-ray Synchrotron Radiation from Electron Beam Slices

separate type		Flux/pulse <sup>a</sup> [photons/0.1%bw]	Flux <sup>b</sup> [photons/sec/0.1%bw]	Peak Intensity [photons/sec/0.1%bw/mm <sup>2</sup> ]	SNR	$\tau^c$ [fs]
90°	spatial+angular	$10 \times 10^3$	$10 \times 10^8$	$2.1 \times 10^{10}$	12	320
	spatial	$18 \times 10^3$	$18 \times 10^8$	$6.5 \times 10^{10}$	5	320
45°	spatial+angular	$5 \times 10^3$	$5 \times 10^8$	$1.1 \times 10^{10}$	8 <sup>d</sup> (2.6)	150
	spatial	$5 \times 10^3$	$5 \times 10^8$	$3.6 \times 10^{10}$	8 <sup>e</sup> (2.7)	150

<sup>a</sup> assume NSLS-II's revolution time is about 2.6  $\mu$ s, then Flux/pulse= Power $\times$ 2.6  $\mu$ s

<sup>b</sup> assume the repetition rate of the low energy linac is 100 kHz, then Flux=Flux/pulse $\times$ 100 kHz

<sup>c</sup> radiation pulse length

<sup>d</sup> with 10 ps of the detector's time resolution

<sup>e</sup> with 10 ps of the detector's time resolution

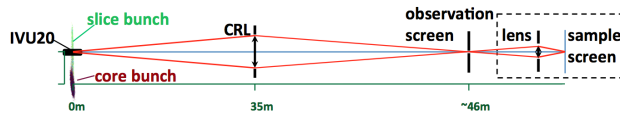


Figure 6: Optical scheme of e-beam slicing beamline.

### Radiation Separation

The thin slice bunch and core bunch pass through the 3 m long U20 in-vacuum undulator and radiate x-ray pulses of length 150 fs–320 fs (depending on the crossing angle) and 30 ps respectively. Due to the spatial and angular differences in vertical phase space of the two bunches, the very short, satellite hard x-ray radiation can be separated from the core bunch radiation with sufficient signal to noise ratio (SNR). We propose a conceptual optical scheme [23] shown in Fig. 6 allowing for the separation of the satellite radiation from the core. To get reliable estimates of the separation performances, a wavefront propagation study was performed using the Synchrotron Radiation Workshop (SRW) physical optics computer code [24].

Two methods are used to separate the radiations. One is the pure spatial separation, and the other one is the spatial and angular hybrid separation [13]. The separate performances on the observation screen is shown in Table. 3. For example, at 90° crossing angle, using spatial and angular hybrid separation, the separate SNR is 12 and the flux per pulse reaches 10000 photons/0.1%BW at the expense of relatively longer 320 fs pulse length. Since the repetition rate can reach 100 kHz, the average flux per second for this case can reach  $1 \times 10^9$  photons/sec/0.1%BW. At 45° crossing angle, the satellite hard x-ray pulse 150 fs is much shorter. The smaller angular kick results in a smaller SNR at 2.7. However, if a fast detector with a time resolution around several picoseconds is used in the femtosecond x-ray diffraction experiment, SNR can increase significantly [13].

### CONCLUSION

These results presented have clearly confirmed the feasibility of electron beam slicing approach as a new method of

the generation of short x-ray pulses. Experimental tests are scheduled in the next future.

### REFERENCES

- [1] A. Zholents, M. Zolotarev, "Femtosecond x-ray pulses of synchrotron radiation" *Phys. Rev. Lett.* **76**, 916 (1996)
- [2] R.W. Schoenlain et al., "Generation of femtosecond pulses of synchrotron radiation" *Science* **287**, 2237 (2000)
- [3] S. Khan et al., "Femtosecond undulator radiation from sliced electron bunches" *Phys. Rev. Lett.* **97**, 074801 (2006)
- [4] G. Ingold et al., "Sub-picosecond optical pulses at the SLS storage ring" in *Proc. PAC01*, Chicago, IL, USA, 2001, pp. 2656-2658
- [5] C. Steier et al., "Accelerator physics challenges of the fs-slicing upgrade at the ALS", in *Proc. PAC03*, Portland, OR, USA, 2003, pp. 397-399
- [6] O. Chubar, P. Elleaume, "Accurate and efficient computation of synchrotron radiation in the near field region" in *Proc. EPAC98*, Grenoble, France, 1998, pp. 1177-1179
- [7] A. Zholents et al., "Generation of subpicosecond X-ray pulses using RF orbit deflection" *Nucl. Instrum. Methods Phys. Res., Sect. A* **425**, 385 (1999)
- [8] M. Katoh, "Ultra-short pulses of synchrotron radiation on storage rings" *Japan. J. Appl. Phys* **38**, L547 (1999)
- [9] M. Borland, "Simulation and analysis of using deflecting cavities to produce short x-ray pulses with the Advanced Photon Source" *PRSTAB* **8**, 074001 (Mar. 2005)
- [10] P. Emma "First lasing of the LCLS X-ray FEL at 1.5 Å" in *Proc. PAC09*, Vancouver, BC, Canada, 2009, pp. 3115-3119
- [11] J.N. Galayda, The Linac Coherent Light Source Project. No. SLAC-PUB-10115 (Aug, 2002)
- [12] F. Willeke, L.H. Yu, "Ultra-short x-ray pulses generation by electron beam slicing in storage rings" in *Proc. IPAC13*, Shanghai, China, 2013, pp. 1134-1136
- [13] A. He, F. Willeke, L.H. Yu, "Ultra-short x-ray pulses generation by electron beam slicing in storage rings" *PRSTAB* **17**, 040701 (2014)
- [14] A. He, F. Willeke, L.H. Yu, "Dependence on crossing angle of electron beam slicing in storage rings" to be submitted

- [15] A. He et al., “Simulation design of a low energy bunch compressor with space charge effect” in Proc. *IPAC13*, Shanghai, China, 2013, pp. 2307-2309
- [16] F. Sannibale et al., “Status of the APEX project at LBNL” in Proc. *IPAC12*, New Orleans, LA, USA, 2012, pp. 2173-2175
- [17] J. Qiang, ImpactT code, LBNL-62326 (2007)
- [18] M. Ehrgott, *Multicriteria Optimization*, (Springer, 2005)
- [19] A. He et al., “Low energy compressor design with high repetition rate for e-beam slicing” in *These Proceedings: Proc. FEL14*, Basel, Switzerland, 2014, THP036
- [20] S. Ozaki et al., “Philosophy for NSLS-II design with sub-nanometer horizontal emittance” in Proc. *PAC07*, Albuquerque, NM, USA, 2007, pp. 77-79
- [21] F. Lohl et al., “Electron bunch timing with femtosecond precision in a superconducting free-electron laser” *Phys. Rev. Lett.* **104**, 144801 (2010)
- [22] M. Borland, ANL APS Report No. LS-287 (2000)
- [23] A. He et al., “Separation of hard X-ray synchrotron radiation from electron beam slices” in Proc. *SPIE Optics + Photonics 2014*, San Diego, California
- [24] O. Chubar et al., “Physical optics computer code optimized for synchrotron radiation” in Proc. *SPIE 4769*, Seattle, WA, USA, 2002, pp. 145-151